SUPPLEMENTARY MATERIAL

This section contains supplementary materials referenced in the main manuscript. All other materials relevant to this study—including code, raw microtextural data, and SEM images— are available at https://github.com/jreahl/Reahl_2020.

Figure S1. Photograph of the Wilsonbreen Formation in Buldrevågen, with a Norwegian 5 kroner piece for scale (26 mm diameter) (© K.D. Bergmann 2017). Note the green-brown color of the unit.

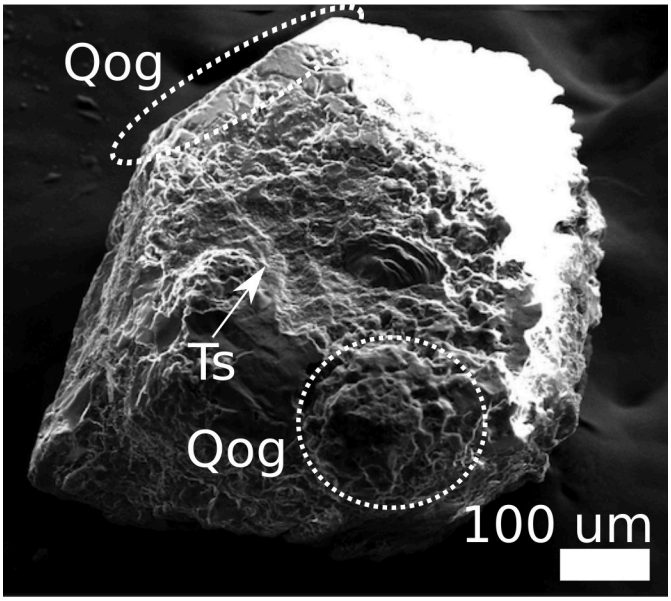

Figure S2. Example of a diagenetically overprinted grain with quartz overgrowths (Qog) and turtle-skin silica (Ts). Because quartz overgrowths and turtle-skin silica overprint the original character of the grains, diagenetically-overprinted grains are excluded from SEM analysis.

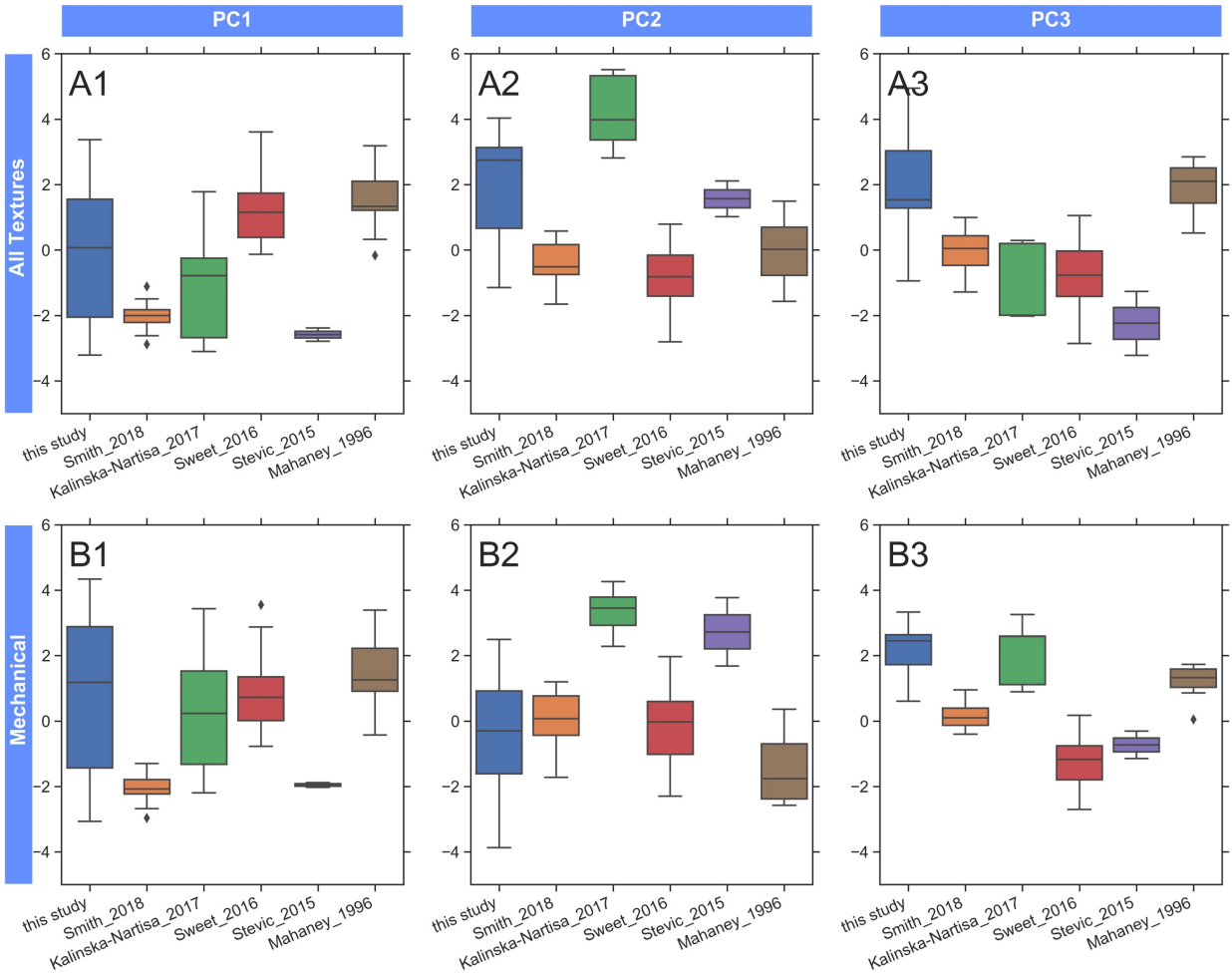

Figure S3. Boxplots of the modern samples grouped by author in the all-textures PCA ordination (row A) and the mechanical ordination (row B). Each column represents a principal component axis in each ordination: PC1 (column 1), PC2 (column 2), and PC3 (column 3). The small black diamonds represent modern outliers for each transport mode.

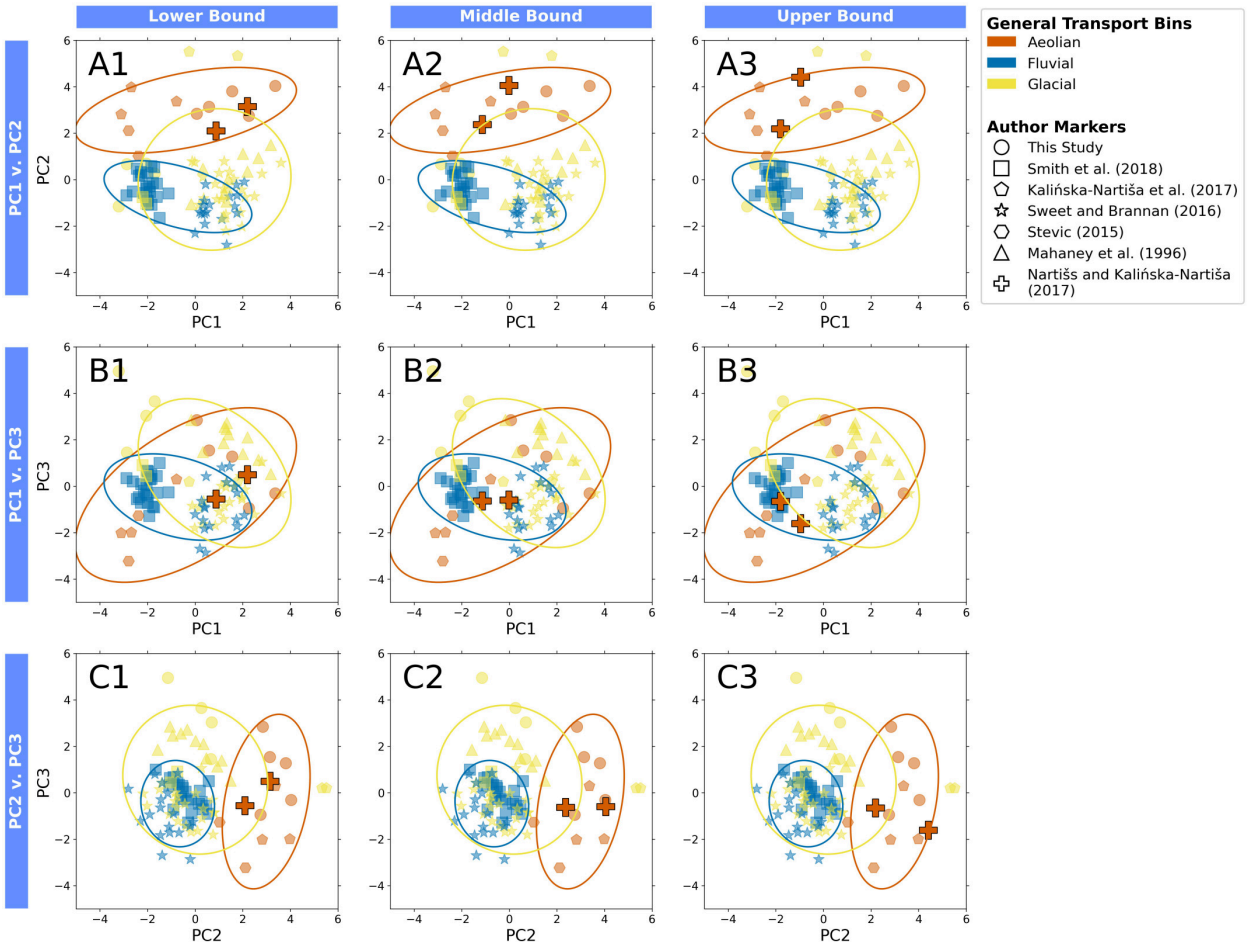

Figure S4. All-textures PCA ordination biplots of the ancient Nartišs and Kalińska-Nartiša (2017) samples using the lower (column 1), middle (column 2), and upper bounds (column 3) of each abundance bin in Nartišs and Kalińska-Nartiša (2017). Row A is in PC1-PC2 space, row B is in PC1-PC3 space, and row C is in PC2-PC3 space. The transparent points represent the modern samples used in this study (this study through Mahaney et al. 1996). The ellipses are 95% confidence intervals of each modern transport mode that are centered at the mean of the transport mode in each coordinate space. The ellipses are calculated using the methods of Schelp (2019).

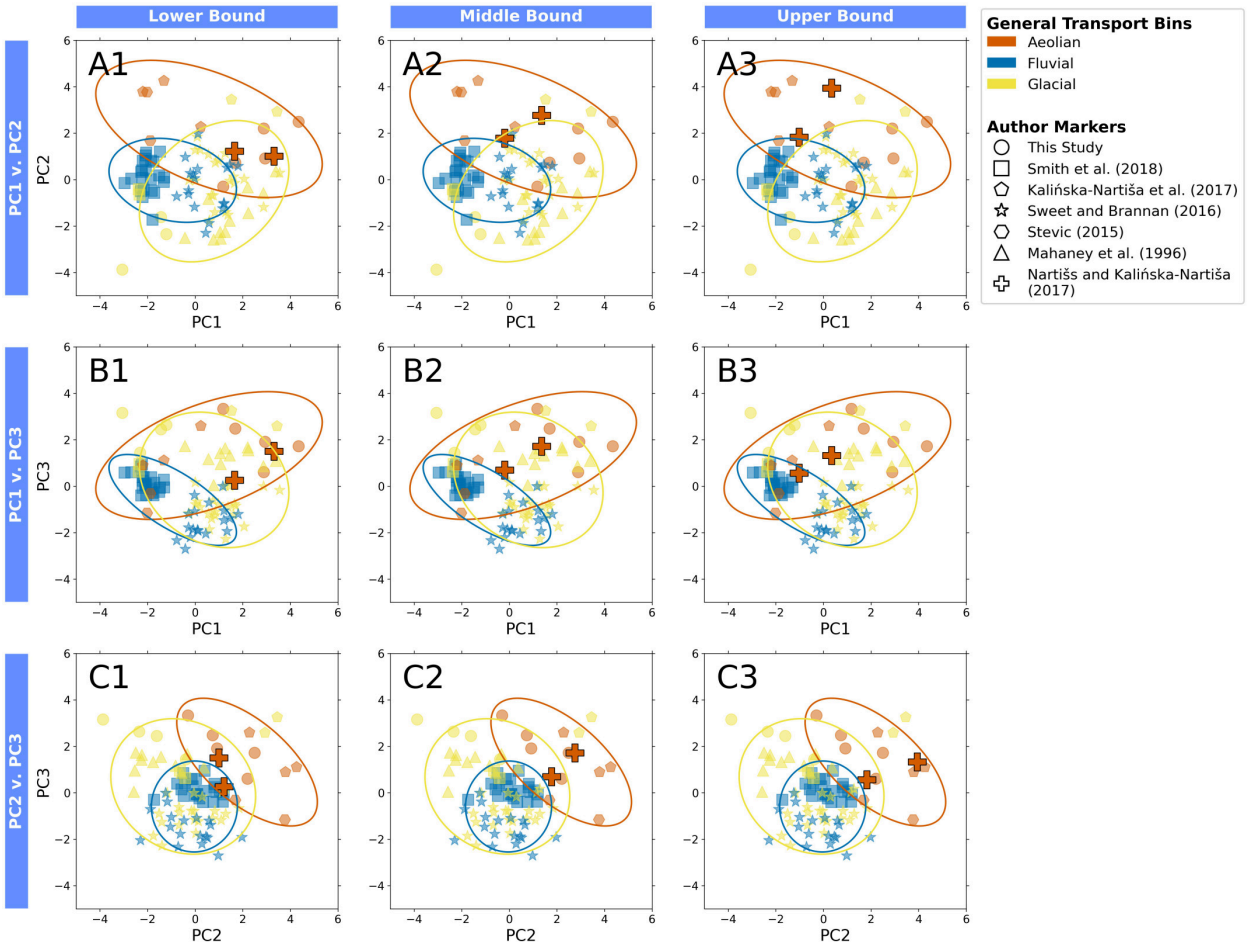

Figure S5. Mechanical PCA ordination biplots of the ancient Nartišs and Kalińska-Nartiša (2017) samples using the lower (column 1), middle (column 2), and upper bounds (column 3) of each abundance bin in Nartišs and Kalińska-Nartiša (2017). Row A is in PC1-PC2 space, row B is in PC1-PC3 space, and row C is in PC2-PC3 space. The transparent points represent the modern samples used in this study (this study through Mahaney et al. 1996). The ellipses are 95% confidence intervals of each modern transport mode that are centered at the mean of the transport mode in each coordinate space. The ellipses are calculated using the methods of Schelp (2019).

Table S1. Microtextural comparison table of all the studies with modern samples considered in this work. Microtextures with no analog to the microtextures analyzed in this study are marked with "N/A".

Citation		This study	Smith et al. (2018)	Kalińska-Nartiša et al. (2017)	Sweet and Brannan (2016)	Stevic (2015)	Mahaney et al. (1996)
Microtexture Analogs	Polygenetic	abrasion features	abrasion features	abrasion fatigue	N/A	abraded edges	abrasion features
		arc-shaped steps	arc-shaped steps	arcuate steps	arc-shaped steps	arcuate steps	arc-shaped steps
		breakage blocks	breakage blocks	breakage blocks	breakage blocks	breakage blocks small	N/A
		conchoidal fractures	conchoidal fractures	conchoidal fractures <100	conchoidal fractures	conchoidal (<100μm)	conchoidal fractures
		fracture faces	fracture faces	N/A	fracture faces	flat cleavage surfaces	fracture faces
		linear steps	linear steps	straight steps	linear steps	straight steps	linear steps
		sharp angular features	sharp angular features	angular grains	sharp angular features	angular	sharp angular features
		subparallel linear fractures	subparallel linear fractures	parallel striations	subparallel linear fractures	parallel striations	subparallel linear fractures
		upturned plates	upturned plates	N/A	mechanically upturned plates	upturned plates	mechanically upturned plates
	Percussion	edge rounding	edge rounding	bulbous edges	edge rounding	bulbous edges	edge rounding
		v-shaped percussion cracks	v-shaped percussion cracks	v-shaped cracks	v-shaped cracks	v-shaped cracks	v-shaped percussion cracks
	High-Stress	crescentic gouges	crescentic gouges	N/A	crescentic gouges	N/A	crescentic gouges
		curved grooves	curved grooves	straight/curved grooves	curved grooves	straight/curved grooves	curved grooves
		deep troughs	deep troughs	N/A	deep troughs	N/A	deep troughs
		straight grooves	straight grooves	N/A	straight grooves	N/A	straight grooves
	Chemical	dissolution etching precipitation features	dissolution etching precipitation features	solution pits precipitation	N/A precipitation features	solution pits precipitation	dissolution etching precipitation features
	General	low relief	low relief	low relief	low relief	low relief	low relief
		medium relief	medium relief	medium relief	medium relief	medium relief	medium relief
		high relief	high relief	high relief	high relief	high relief	high relief

Table S2. Microtextural comparison table of all the studies with ancient samples considered in this work. Microtextures with no analog to the microtextures analyzed in this study are marked with "N/A".

Citation		This study	Nartišs and Kalińska-Nartiša (2017)	Deane (2010)	Sweet and Soreghan (2010)	Mahaney et al. (2001)	Mahaney and Kalm (1995)
Microtexture Analogs	Polygenetic	abrasion features	abrasion fatigue	abrasion	abrasion features	abrasion features	abrasion features
		arc-shaped steps	arcuate steps	arc-shaped steps	arc-shaped steps	arc-shaped steps	arc-shaped steps
		breakage blocks	N/A	breakage blocks	breakage blocks	N/A	N/A
		conchoidal fractures	conchoidal features (<100μm)	conchoidal fractures	conchoidal fractures	conchoidal fractures	conchoidal fractures
		fracture faces	N/A	fracture faces	fracture faces	fracture faces	fracture faces
		linear steps	straight steps	linear steps	linear steps	linear steps	linear steps
		sharp angular features	angular outline	sharp, angular features	sharp angular features	sharp angular features	sharp angular features
		subparallel linear fractures	parallel striations	sub-parallel linear fractures	subparallel linear fractures	subparallel linear fractures	subparallel linear fractures
		upturned plates	upturned plates	mechanically upturned plates	mechanically upturned plates	mechanically upturned plates	mechanically-upturned plates
	Percussion	edge rounding	bulbous edges	edge rounding	edge rounding	edge rounding	edge rounding
		v-shaped percussion cracks	v-shaped percussion cracks	v-shaped percussion fractures	v-shaped percussion cracks	v-shaped percussion cracks	v-shaped percussion cracks
	High-Stress	crescentic gouges	N/A	crescentic gouges	crescentic gouges	crescentic gouges	crescentic gouges
		curved grooves	straight/curved grooves	curved grooves	curved grooves	curved grooves	curved grooves
		deep troughs	N/A	deep troughs	deep troughs	deep troughs	deep troughs
		straight grooves	N/A	straight grooves	straight grooves	straight grooves	straight grooves
	Chemical	dissolution etching	solution pits	dissolution etching	dissolution etching	dissolution etching	dissolution etching
		precipitation features	precipitation	precipitation	N/A	precipitation features	precipitation features
	General	low relief	low relief	low relief	low relief	low relief	low relief
		medium relief	medium relief	medium relief	medium relief	medium relief	medium relief
		high relief	high relief	high relief	high relief	high relief	high relief

Table S3. First quartiles (q25), medians (q50), third quartiles (q75), lower adjacent values (h1), and upper adjacent values (h2) of modern aeolian, fluvial, and glacial samples along PC1, PC2, and PC3 in the all-textures and mechanical PCA ordinations.

Ordination	PC	Transport Mode	q25	q50	q75	h1	h2
All Textures	PC1	Aeolian	-2.6	-0.4	1.3	-3.1	3.4
		Fluvial	-2.0	-1.6	0.4	-2.9	2.1
		Glacial	0.2	1.2	1.9	-2.2	3.6
	PC2	Aeolian	2.8	3.0	3.7	2.1	4.0
		Fluvial	-1.2	-0.7	-0.2	-2.3	0.6
		Glacial	-0.8	-0.2	0.7	-2.2	1.5
	PC3	Aeolian	-1.8	-0.6	1.0	-3.2	2.8
		Fluvial	-0.9	-0.4	0.3	-2.7	1.0
		Glacial	-0.6	0.2	1.5	-1.8	3.7
Mechanical	PC1	Aeolian	-1.7	0.7	2.6	-2.2	4.3
		Fluvial	-2.1	-1.5	0.0	-3.0	1.8
		Glacial	0.1	1.0	1.6	-1.4	3.6
	PC2	Aeolian	1.1	2.2	3.4	-0.3	4.3
		Fluvial	-0.6	0.1	0.6	-2.3	2.0
		Glacial	-1.5	-0.6	0.3	-3.9	2.9
	PC3	Aeolian	0.7	1.4	2.3	-1.1	3.3
		Fluvial	-1.4	-0.3	0.1	-2.7	0.9
		Glacial	-0.9	0.0	1.4	-2.3	3.3

Table S4. First quartiles (q25), medians (q50), third quartiles (q75), lower adjacent values (h1), and upper adjacent values (h2) of the modern samples grouped by study along PC1, PC2, and PC3 in the all-textures and mechanical PCA ordinations.

type	PC	Study	q25	q50	q75	h1	h2
All Textures	PC1	this study	-2.1	0.1	1.6	-3.2	3.4
		Smith et al. (2018)	-2.2	-2.0	-1.8	-2.6	-1.5
		Kalińska-Nartiša et al. (2017)	-2.7	-0.8	-0.3	-3.1	1.8
		Sweet and Brannan (2016)	0.4	1.2	1.7	-0.1	3.6
		Stevic (2015)	-2.7	-2.6	-2.5	-2.8	-2.4
		Mahaney et al. (1996)	1.2	1.3	2.1	0.3	3.2
	PC2	this study	0.7	2.7	3.1	-1.2	4.0
		Smith et al. (2018)	-0.8	-0.5	0.2	-1.7	0.6
		Kalińska-Nartiša et al. (2017)	3.4	4.0	5.3	2.8	5.5
		Sweet and Brannan (2016)	-1.4	-0.8	-0.2	-2.8	0.8
		Stevic_2015	1.3	1.6	1.8	1.0	2.1
		Mahaney et al. (1996)	-0.8	0.0	0.7	-1.6	1.5
	PC3	this study	1.3	1.5	3.0	-0.9	4.9
		Smith et al. (2018)	-0.5	0.0	0.4	-1.3	1.0
		Kalińska-Nartiša et al. (2017)	-2.0	0.2	0.2	-2.0	0.3
		Sweet and Brannan (2016)	-1.4	-0.8	0.0	-2.9	1.1
		Stevic (2015)	-2.7	-2.2	-1.8	-3.2	-1.3
		Mahaney et al. (1996)	1.4	2.1	2.5	0.5	2.8
Mechanical	PC1	this study	-1.4	1.2	2.9	-3.1	4.3
		Smith et al. (2018)	-2.2	-2.1	-1.8	-2.7	-1.3
		Kalińska-Nartiša et al. (2017)	-1.3	0.2	1.5	-2.2	3.4
		Sweet and Brannan (2016)	0.0	0.7	1.3	-0.8	2.9
		Stevic (2015)	-2.0	-2.0	-1.9	-2.0	-1.9
		Mahaney et al. (1996)	0.9	1.3	2.2	-0.4	3.4
	PC2	this study	-1.6	-0.3	0.9	-3.9	2.5
		Smith et al. (2018)	-0.4	0.1	0.8	-1.7	1.2
		Kalińska-Nartiša et al. (2017)	2.9	3.4	3.8	2.3	4.3
		Sweet and Brannan (2016)	-1.0	0.0	0.6	-2.3	2.0
		Stevic (2015)	2.2	2.7	3.2	1.7	3.8
		Mahaney et al. (1996)	-2.4	-1.8	-0.7	-2.6	0.4
	PC3	this study	1.7	2.4	2.6	0.6	3.3
		Smith et al. (2018)	-0.1	0.1	0.4	-0.4	1.0
		Kalińska-Nartiša et al. (2017)	1.1	2.6	2.6	0.9	3.3
		Sweet and Brannan (2016)	-1.8	-1.2	-0.8	-2.7	0.2
		Stevic (2015)	-0.9	-0.7	-0.5	-1.1	-0.3
		Mahaney et al. (1996)	1.0	1.3	1.6	0.9	1.7